JHEP|Reports

Oncogenic role of PMEPA1 and its association with immune exhaustion and TGF-β activation in HCC

Authors

Marta Piqué-Gili, Carmen Andreu-Oller, Agavni Mesropian, …, Amaia Lujambio, Roser Pinyol, Josep M. Llovet

Correspondence

jmllovet@clinic.cat (J.M. Llovet).

Graphical abstract

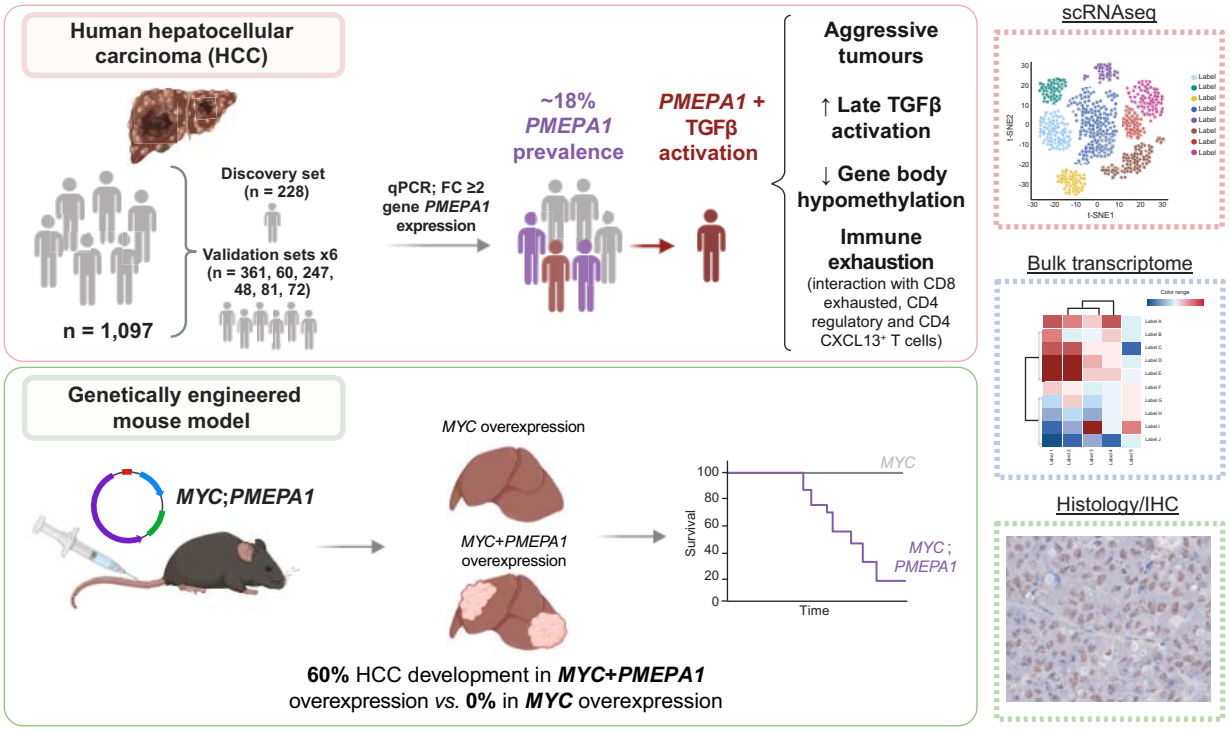

Highlights:

- *PMEPA1* is overexpressed in 18% of human HCCs and is expressed by both tumoural and stromal cell populations.
- Overexpression of *PMEPA1* combined with TGF-β activation is present in 12% of human HCCs.
- *PMEPA1*^{High}/TGF-β-active status is associated with tumour aggression and an immunosuppressive tumour microenvironment.
- *In vivo*, overexpression of *MYC*+*PMEPA1* led to HCC development in ∼60% of cases (*vs.* 0% in *MYC* alone).

Impact and implications:

PMEPA1 can enhance the tumour-promoting effects of TGF-β in cancer. In this study, we demonstrate that *PMEPA1* is highly expressed in ∼18% of patients with hepatocellular carcinoma (HCC), a feature associated with poor prognosis, TGF-β activation and exhaustion of immune cells. Similarly, in mouse models, *PMEPA1* overexpression promotes HCC development, which demonstrates its oncogenic role. The identification of *PMEPA1* as oncogenic driver in HCC and its role in immune exhaustion and poor clinical outcomes enhances our understanding of HCC pathogenesis and opens new avenues for targeted therapeutic interventions.

https://doi.org/10.1016/j.jhepr.2024.101212

JHEP|Reports

Oncogenic role of PMEPA1 and its association with immune exhaustion and TGF-β activation in HCC☆

Marta Piqué-Gili[1,†], **Carmen Andreu-Oller**[1,†], **Agavni Mesropian**[1,†], Roger Esteban-Fabró[1], Marina Bárcena-Varela[2], Marina Ruiz de Galarreta[2], Carla Montironi[1,3], Iris Martinez-Quetglas[1], Sarah Cappuyns[4,5,6,7], Judit Peix[1], Ieva Keraite[2], Albert Gris-Oliver[1], Elisa Fernández-Martínez[2], Ezequiel Mauro[1], Miguel Torres-Martin[1], Jordi Abril-Fornaguera[1], Katherine E. Lindblad[2], Diether Lambrechts[6,7], Jeroen Dekervel[4,5], Swan N. Thung[2], Daniela Sia[2], Amaia Lujambio[2], Roser Pinyol[1], Josep M. Llovet[1,2,8,*]

JHEP Reports **2024**. vol. 6 | 1–14

Background & Aims: Transforming growth factor β (TGF-β) plays an oncogenic role in advanced cancer by promoting cell proliferation, metastasis and immunosuppression. *PMEPA1* (prostate transmembrane protein androgen induced 1) has been shown to promote TGF-β oncogenic effects in other tumour types. Thus, we aimed to explore the role of *PMEPA1* in hepatocellular carcinoma (HCC).

Methods: We analysed 1,097 tumours from patients with HCC, including discovery (n = 228) and validation (n = 361) cohorts with genomic and clinicopathological data. *PMEPA1* levels were assessed by qPCR (n = 228), gene expression data (n = 869) and at the single-cell level (n = 54). Genetically engineered mouse models overexpressing *MYC*+*PMEPA1* compared to *MYC* were generated and molecular analyses were performed on the HCCs obtained.

Results: *PMEPA1* was overexpressed in 18% of HCC samples (fold-change >2; n = 201/1,097), a feature associated with TGF-β signalling activation (p <0.05) and absence of gene body hypomethylation (p <0.01). HCCs showing both TGF-β signalling and high *PMEPA1* levels (12% of cases) were linked to immune exhaustion, late TGF-β activation, aggressiveness and higher recurrence rates after resection, in contrast to HCCs with only TGF-β signalling (8%) or *PMEPA1* overexpression (9%). Single-cell RNA sequencing analysis identified *PMEPA1* expression in HCC and stromal cells. *PMEPA1*-expressing tumoural cells were predicted to interact with $CD4^+$ regulatory T cells and $CD4^+$ $CXCL13^+$ and $CD8^+$ exhausted T cells. *In vivo*, overexpression of *MYC*+*PMEPA1* led to HCC development in ∼60% of mice and a decreased survival compared to mice overexpressing *MYC* alone (p = 0.014). *MYC*+*PMEPA1* tumours were enriched in TGF-β signalling, paralleling our human data.

Conclusions: In human HCC, *PMEPA1* upregulation is linked to TGF-β activation, immune exhaustion, and an aggressive phenotype. Overexpression of *PMEPA1*+*MYC* led to tumoural development *in vivo*, demonstrating the oncogenic role of *PMEPA1* in HCC for the first time.

Introduction

Liver cancer represents the third leading cause of cancer-related death worldwide, and the number of new cases and deaths is projected to rise to >55% by 2040.[1,2] Hepatocellular carcinoma (HCC) accounts for approximately 90% of primary liver cancer cases, with 50 to 60% of patients with HCC currently being exposed to systemic therapies. Although our understanding of the pathophysiology and drivers of the disease has improved over the past years, HCC tumours present few actionable mutations (overall ∼20% tumours have an actionable target), and the translation of molecular knowledge into precision oncology remains a challenge.[3,4] Consequently, the identification of actionable molecular determinants of HCC remains an unmet need.

Previous studies examining genomic, transcriptomic and epigenomic features have established two distinct molecular classes of HCC, each accounting for approximately 50% of cases.[2,5] The proliferation class is characterized by poorly differentiated tumours exhibiting high vascular invasion and poor clinical outcomes, and can be subdivided into the S1 and S2 subclasses.[2] S1-class tumours are distinguished by transforming growth factor β (TGF-β)-activated Wnt signalling, while S2-class tumours display progenitor cell features.[6,7] In contrast, HCCs of the non-proliferation subclass (also known

☆ Given their role as Editor, Josep M. Llovet had no involvement in the peer-review of this article and had no access to information regarding its peer-review. Full responsibility for the editorial process for this article was delegated to the Guest Editor Jessica Zucman-Rossi.

* Corresponding author. Address: Translational Research in Hepatic Oncology Group, Liver Unit, IDIBAPS-Hospital Clinic, University of Barcelona, C/Rosselló 153, 08036, Barcelona, Catalonia, Spain. Tel.: 34-93-227-9155.
E-mail address: jmllovet@clinic.cat (J.M. Llovet).
† These authors contributed equally to this work

https://doi.org/10.1016/j.jhepr.2024.101212

as S3) present less aggressive features, with an enrichment of *CTNNB1* mutations and activation of interferon signalling.[2]

From an immunological standpoint, HCCs can be classifed into inflamed (~35%) and non-inflamed (~65%).[5,8] Inflamed tumours exhibit high immune T cell infiltration, cytolytic activity and interferon signalling, and can be further divided into immune-active, immune-exhausted, and immune-like subclasses. Notably, the immune-exhausted subclass is enriched in TGF-β signalling,[9] a defining feature of the S1 proliferation subclass of HCC and a crucial player in hepatocarcinogenesis.[10]

TGF-β signalling plays a complex and highly contextual role, both in HCC and other tumour types.[11] In premalignant cells, TGF-β exhibits cytostatic effects,[12] while in advanced stages, it contributes to tumour progression and metastasis by inducing epithelial-mesenchymal transition (EMT), thereby enhancing cell migration and invasion.[13,14] Also, TGF-β has been reported to mediate immune evasion and immune suppression within the tumour microenvironment (TME) and contributes to immunotherapy resistance across various tumour types.[15,16]

In HCC, several gene signatures recapitulate TGF-β signalling. On one hand, the Wnt-TGF-β signature is associated with TGF-β activation in HCC, along with features of poor outcome.[17] On the other hand, the Late TGF-β signature captures the TGF-β oncogenic effects and is associated with an invasive phenotype and worse clinical outcomes, while the Early TGF-β signature is associated with the tumour-suppressive functions of TGF-β and a better clinical prognosis.[18] Both Wnt-TGF-β and Late TGF-β signatures are enriched in immune-exhausted HCCs.[8] These tumours also overexpress prostate transmembrane protein androgen induced 1 (*PMEPA1*),[9] a direct target gene and regulator of the TGF-β pathway.[19]

The oncogenic or tumour-suppressive functions of *PMEPA1* are cancer-type specific. While *PMEPA1* has been shown to promote the TGF-β oncogenic effects through non-canonical PI3K/AKT signalling in breast and colorectal cancer,[20–22] it has also been reported to regulate TGF-β to prevent bone metastasis in prostate cancer.[19] In HCC, high *PMEPA1* levels correlate with poor prognosis and targeting *PMEPA1* inhibits the migration of TGF-β1-activated murine HCC cells.[23] Nonetheless, the role of *PMEPA1* and its interplay with TGF-β signalling in human and murine HCC remains poorly understood.

This study analysed *PMEPA1* expression levels in 1,097 human HCC samples, revealing its overexpression in 18% of tumours. Through a comprehensive -omics analysis we demonstrated that the activation of TGF-β signalling in the context of *PMEPA1* overexpression is associated with poor prognosis features and immune exhaustion. Single-cell RNA sequencing (scRNAseq) data analysis uncovered a key contribution of the surrounding stromal microenvironment to *PMEPA1* overexpression. Importantly, we demonstrated that *PMEPA1* is an oncogene using an *in vivo* model of HCC. The results of the transcriptomic analysis of murine tumours paralleled our human HCC data.

Materials and methods

HCC human samples and transcriptomic/genomic data

Gene expression profiles from a total of 1,097 human HCC samples were analysed (Table S1), including a training set of 228 fresh frozen HCCs from patients who underwent liver resection (Heptromic dataset; GSE63898)[24] and six validation cohorts comprising a total of 508 publicly available HCC cases (GSE64041,[25] GSE14520,[26,27] GSE45267,[28] GSE62232[3] and GSE39791[29]) and 361 HCCs from The Cancer Genome Atlas (TCGA) database (https://tcga-data.nci.nih.gov/). Single nucleotide polymorphism array data were available for the Heptromic cohort.[30] *PMEPA1* mRNA levels were measured by quantitative reverse-transcription PCR in 228 tumours of the Heptromic cohort. TCGA protein array (RPPA) data were downloaded from the GDC Data Portal.

The GenePattern modules Nearest Template Prediction (NTP) and single-sample gene set-enrichment analysis were used to evaluate gene signatures representing TGF-β pathway activation, as well as previously reported HCC subclasses. For NTP analyses, significance was defined using Benjamini-Hochberg false discovery rate <0.05, or <0.25 in the case of the Wnt-TGF-β subclass.[7]

Gene signatures used in the analyses are listed in Table S2, or were retrieved from the Molecular Signatures Database (MSigDB) resource (www.broadinstitute.org/msigdb). Immune deconvolution tools implemented in TIMER2.0[31] were used to estimate the relative fraction of immune and stromal cells infiltrating the tumour. To identify differentially expressed genes (DEGs) between groups of samples, we performed moderated t-tests using the eBayes function of the R package *limma* (v '3.54.2'). DEGs were selected based on p values <0.05 and $\log_2$ fold-change >2. The Enrichr tool[32] was used to evaluate enrichment in specific pathways and biological functions among the DEGs.

Analysis of the methylation status of *PMEPA1*

Methylation array data were available for the Heptromic cohort and human HCC cell lines and published elsewhere.[24,30] Methylation array data from the TCGA cohort (n = 361 samples) were downloaded from the UCSC Xena Browser (https://xenabrowser.net). To study the differential methylation status of *PMEPA1* between HCC and non-cancerous liver tissue, we used array probes located at the promoter and gene body (transcript variant 1; NM_020182; Table S3). Hypomethylation and hypermethylation per sample were defined as the mean fold-change compared to non-tumour tissue ± 2 SD.

For details on microRNA profiling and analysis, please refer to the supplementary methods.

Single-cell analysis of human HCC samples

Single-cell RNAseq data from a cohort of 38 human HCCs were available from previous work.[33] Additionally, single-cell RNA-seq data from 32 human HCCs were downloaded from Gene Expression Omnibus (GSE151530). Both single-cell RNAseq datasets were analysed in the same way using the Seurat package (version 4.1.0) from R (version 4.2.0). First, we quality-filtered cells with more than 100 and less than 6,000 detected genes, less than 50% of mitochondrial RNA and with unique molecular identifier counts greater than 400. We also excluded those samples with less than 200 cells in total, and those obtained after treatment, retaining a total of 38 and 16 HCC samples for the final analyses. The total number of transcripts in each single cell was normalized to 10,000 and log-transformed. Subsequently, the top 2,000 highly variable genes were detected according to average expression (0.05 to

3) and dispersion (>0.5), and data was scaled using a linear model and regressing out the total RNA count, the percentage of mitochondrial genes and the cell cycle state (S and G2M scores). The detected variable genes were then considered as the main drivers of cell-to-cell differences and were used for principal component analysis. Then, data integration across samples was performed using Harmony (version 0.1.0),[34] and the first 30 Harmony embeddings were used to cluster the cells by calculating K-nearest neighbours and applying the Louvain modularity optimization algorithm. Annotation of malignant *vs.* non-malignant cells was based on differentially expressed marker genes exposed in Table S4. More detailed annotation of NK cells, CD8 T cells and CD4 T cells was performed by subsetting these populations from the quality-filtered Seurat object before normalizing the expression data, clustering and annotating using the differentially expressed marker genes from Table S4 (same parameters as above). Finally, annotation of *PMEPA1*-positive (*PMEPA1*$^+$) cells was based on an expression level of *PMEPA1* higher than 0. The ligand-receptor interactions between *PMEPA1*$^+$ tumour/stromal cells and CD8$^+$ exhausted T cells, CD4$^+$ regulatory T cells and CD4$^+$ CXCL13$^+$ T cells were obtained with CellChat (v1.1.3) algorithm[35] as previously reported.[33]

Reverse-transcription PCR and quantitative reverse-transcription PCR

Total RNA was extracted from HCC tissue using the RNeasy Mini Kit (Qiagen). 1 μg of RNA was retrotranscribed to cDNA using the High-Capacity cDNA Reverse Transcription Kit (Applied Biosystems, Waltham, MA). For relative mRNA quantification, TaqMan® Gene Expression Assays were used following the manufacturer's instructions (Applied Biosystems). Relative quantification was calculated using the ΔΔCq method and normalized based on 18S. The TaqMan® probes used in the assay were Hs00375306_m1 (human PMEPA1) and Hs99999901_s1 (18S).

To quantify *PMEPA1* in cells, total RNA was extracted from cells collected at 80% confluence using the RNeasy Mini Kit (Qiagen) and retrotranscribed and quantified as described.

Cell lines and cell viability assay

Hep3B, PLC5, SNU182, SNU387, SNU398, SNU423 and SNU449 HCC cell lines were obtained from the ATCC, while the Huh7 cell line was purchased from the Japanese Collection of Research Bioresources. Cell lines were regularly confirmed to be mycoplasma free using EZ-PCR kit (Biological Industries, Kibbutz Beit Haemek, Israel). HCC cell lines were cultured in DMEM or RPMI (ThermoFisher, Waltham, MA) supplemented with 10% heat-inactivated FBS.

For the cell viability assay, cells were seeded in 96-well plates and incubated with 5 ng/ml of recombinant human TGF-β1 ligand (Prepotech, Rocky Hill, NJ) for 3 days in humidified atmosphere at 37 °C and 5% CO_2. Cell viability was determined by 3-(4,5-dimethylthiazol-2-yl)-2,5-diphenyltetrazolium bromide (MTT) dye uptake using the CellTiter 96® Cell Proliferation Kit (Promega, Madison, WI) following the manufacturer's instructions.

For details on HCC cell line transcriptomic analyses, please refer to the supplementary methods.

Animal studies, hydrodynamic tail vein injection, and vector design

All the *in vivo* experiments were performed in 6- to 8-week-old C57BL/6 mice purchased from Envigo (Charlotte, NC). All the animals were healthy and acclimated to the animal facility before experimental use, and all the procedures were approved by the Icahn School of Medicine at Mount Sinai Animal Care and Use Committee (IACUC- 2014-0229). Animals were monitored daily and if moribund were euthanized according to the Guidelines for Human End Points for Animals used in biomedical research.

Transposon-based vectors overexpressing *MYC* (*pT3-EF1a-MYC*) or *PMEPA1* (*pT3-EF1a-PMEPA1*) were prepared as follows. The *CMV-SB13-Luc* and *pT3-EF1a-NRAS-IRES-GFP* vectors were used as backbone for cloning and were kindly provided by Dr Scott Lowe (Memorial Sloan Kettering Cancer Center, New York, NY). The *pT3-EF1a-MYC* vector (Addgene plasmid #92046; Addgene Watertown, MA) was a kind gift from Dr Xin Chen (University of California, San Francisco, San Francisco, CA). *The pT3-EF1A-PMEPA1* vector was prepared using the *pT3-EF1a-NRAS-IRES-GFP* plasmid. It was digested with XhoI and EcoRV restriction enzymes (New England BioLabs, Ipswich, MA) and ligated with human *PMEPA1* amplified from pT3-EF1a-PMEPA1. All constructs were verified by nucleotide sequencing, and vector integrity was confirmed by restriction enzyme digestion.

Vectors overexpressing *MYC* (*pT3-EF1a-MYC*), *PMEPA1* (*pT3-EF1a-PMEPA1*) and the SB13 transposase (*CMV-SB13*) were delivered into the liver of wild-type mice through hydrodynamic tail vein injection. Vectors were injected in a sterile saline solution (Intermountain Life Sciences, West Jordan, UT) containing 10 μg of transposon vectors (pT3-based vector) and 2.5 μg of transposase-encoding vector (SB13). A volume equivalent to 10% of mouse body weight was injected through the tail vein using a 3 ml syringe (Becton Dickinson, San Jose, Calif) with a 26-gauge × 0.625 (Becton Dickinson) needle. The mice were monitored for tumour formation and humanely killed at the end point. The end point was defined either by tumour burden or after a period of 100 days. Liver tissue was collected, fixed in formalin and freshly frozen for histological and molecular characterization.

Transcriptomic analysis of murine HCC samples

Total RNA was extracted from murine HCC tissues using the RNeasy Mini Kit (Qiagen). RNA was poly-A selected and multiplexed RNAseq libraries were prepared using the TruSeq RNA Sample Preparation kit (Illumina, San Diego, CA), according to the manufacturer's instructions, at the Icahn School of Medicine at Mount Sinai Genomics Core. The libraries were quantified using the Qubit Broad Range kit (Thermo Fisher Scientific, Waltham, MA) and sequenced using the Illumina HiSeq 4000 system (SR100). Processing of murine transcriptome data (*i.e.*, normalization, background correction, and filtering) was conducted as previously reported.[36] For comparison purposes, we

also analysed transcriptomic data from healthy liver tissue samples and the previously reported *MYC-luc;CTNNB1* and *MYC-lucOS;p53* models.[36]

Histological and immunohistochemical analyses of human and murine HCC samples

Please refer to the supplementary methods.

Statistical analysis

Statistical analyses were performed using R (version 4.2.2). Comparison of continuous variables was conducted using the Student's *t* test for parametric distributions and the Wilcoxon rank-sum test for non-parametric distributions. Association among categorical variables was analysed using Fisher's exact test. In the event of a multiple comparison testing, Benjamini-Hochberg correction was applied. For the assessment of correlations between two normally distributed continuous variables, we used Pearson correlation coefficient. Impact of PMEPA1 and TGF-β activation on recurrence and survival of the Heptromic and Montironi *et al.*, Gut 2023 cohorts were assessed with Kaplan-Meier estimates and compared using the log-rank test. Univariate and multivariate Cox regressions were used to analyse the association between molecular and clinical-pathological variables with recurrence. Specifically, variables with a p value <0.05 in the univariate analysis were included in the multivariate model.

Results

Identification of *PMEPA1* as a potential driver of TGF-β pathway activation in HCC cell lines

To investigate the oncogenic effects of TGF-β in HCC, we stimulated eight human HCC cell lines with TGF-β1. Based on the changes in cell viability induced by TGF-β1, we classified each cell line as either responsive (n = 3) or resistant (n = 5) to the cytostatic effects of TGF-β1 (Fig. 1A). Differential gene expression analysis between the responsive and resistant conditions revealed that TGF-β-resistant HCC cells exhibit a significant upregulation of genes associated with EMT, cell migration and angiogenesis regulation (Fig. 1B, Table S5). Notably, *PMEPA1* emerged as one of the most highly upregulated genes related to the TGF-β pathway in TGF-β-resistant HCC cells (Fig. 1B). These findings suggest that this subset of cells may exhibit a more oncogenic TGF-β phenotype. Upregulation of *PMEPA1* in these cell lines was confirmed both by reverse-transcription PCR and immunohistochemistry (Fig. S1A,B). These observations prompted us to further explore the role of *PMEPA1* in human HCC.

In human HCC tumours, *PMEPA1* is upregulated and its overexpression is associated with TGF-β signalling, proliferation and immune exhaustion

In human HCC samples, *PMEPA1* was found to be overexpressed (≥2-fold compared to healthy or non-tumoural adjacent tissue, referred to as *PMEPA1*^{High}) in 18% of cases (n = 201/1,097; Fig. 1D, Table S1). Overexpression was confirmed at the protein level in 15 out of 23 human HCC tumours, from which 11 were *PMEPA1*^{High} (Fig. S1C,D). In two independent cohorts, *PMEPA1*^{High} tumours consistently upregulated a set of genes linked to TGF-β signalling, EMT, angiogenesis, cell migration and extracellular matrix organization (Fig 1D and Fig. S2A). At the protein level, *PMEPA1*^{High} tumours expressed high levels of CD31 and vimentin (angiogenesis and EMT), but moderate Ki67 and PD1 (proliferation and exhaustion) (Fig. S2).

Both in our discovery cohort as well as in our validation cohorts, *PMEPA1*^{High} tumours were also significantly enriched in both the Wnt-TGF-β HCC subclass – reported to be associated with a higher risk of recurrence after resection[17] – and the Late TGF-β signature (Fig 1C and Fig. S3) – associated with shorter survival, increased recurrence rates, and a more invasive HCC phenotype.[18] Consistently, *PMEPA1*^{High} tumours belonged to the S1/Proliferation HCC molecular subclass.[6,37] Additionally, *PMEPA1* expression levels were positively correlated with the expression of TGF-β ligands (*TGFβ1*, *TGFβ2* and *TGFβ3;* r = 0.14 to 0.86; p <0.05), and SMAD family members (*SMAD2 and SMAD5;* r = 0.2 to 0.3; p <0.05) (Fig. S4). Interestingly, *PMEPA1*^{High} HCCs presented an absence of the early TGF-β signature – associated with the tumour suppressor effects of TGF-β and better prognosis[18] (p <0.05; Fig. 1C).

From the immunological standpoint, *PMEPA1*^{High} tumours mainly belonged to the Inflamed/Exhausted HCC immune subclasses,[8,9] and exhibited a significant enrichment in active stroma signalling[38] (p <0.05; Fig. 1C), results that were validated in TCGA and a further three cohorts (Fig. S3). *PMEPA1*^{High} tumours were also enriched in TGF-β-response signatures of TME cell populations (fibroblasts, macrophages, endothelial cells and T cells)[39] (Fig. S5A), and *PMEPA1* levels positively correlated with a larger tumour stromal compartment as determined by deconvolution tools (see methods for details; Fig. S5B).

In addition, the CTNNB1 molecular subclass was absent in *PMEPA1*^{High} tumours (Fig 1C and Fig. S3), supported by the fact that *CTNNB1* mutations were significantly less prevalent in samples that overexpress *PMEPA1* (5% in *PMEPA1*^{High} tumours *vs.* 32% in *PMEPA1*^{Low} tumours; p <0.0001; Fig. S6), and consistent with a previously reported role for *PMEPA1* overexpression in interfering with β-catenin stability and nuclear translocation in breast cancer models.[40]

We next assessed whether *PMEPA1* overexpression in HCC could be related to epigenetic deregulation, as described in other tumour types.[41] We assessed the methylation status of the *PMEPA1* promoter and gene body in human HCCs with high or low *PMEPA1* levels and in healthy liver samples. While no differences were observed in terms of promoter methylation between *PMEPA1*^{High} and *PMEPA1*^{Low} tumours, methylation levels in the gene body were reduced in *PMEPA1*^{Low} samples, both in the Heptromic (Fig. 1E) and TCGA (Fig. S7A) datasets. Indeed, the *PMEPA1*^{Low} group displayed a higher proportion of samples with hypomethylation of the gene body (Fig. S7B). This association was confirmed in human HCC cell lines, where we also observed that the methylation levels of CpGs located within the *PMEPA1* gene body were reduced in cells with low *PMEPA1* levels (Hep3B) compared to cell lines overexpressing *PMEPA1* (SNU182, SNU387, SNU398, SNU423 and SNU449) (Fig. S8). This is consistent with the fact that gene body hypomethylation in cancer has been associated with reduced transcription compared to normal cells.[42,43]

Since several microRNAs (miRNAs) have been shown to control *PMEPA1* expression in other tumour types,[44] we went on to analyse whether there was any miRNA associated with

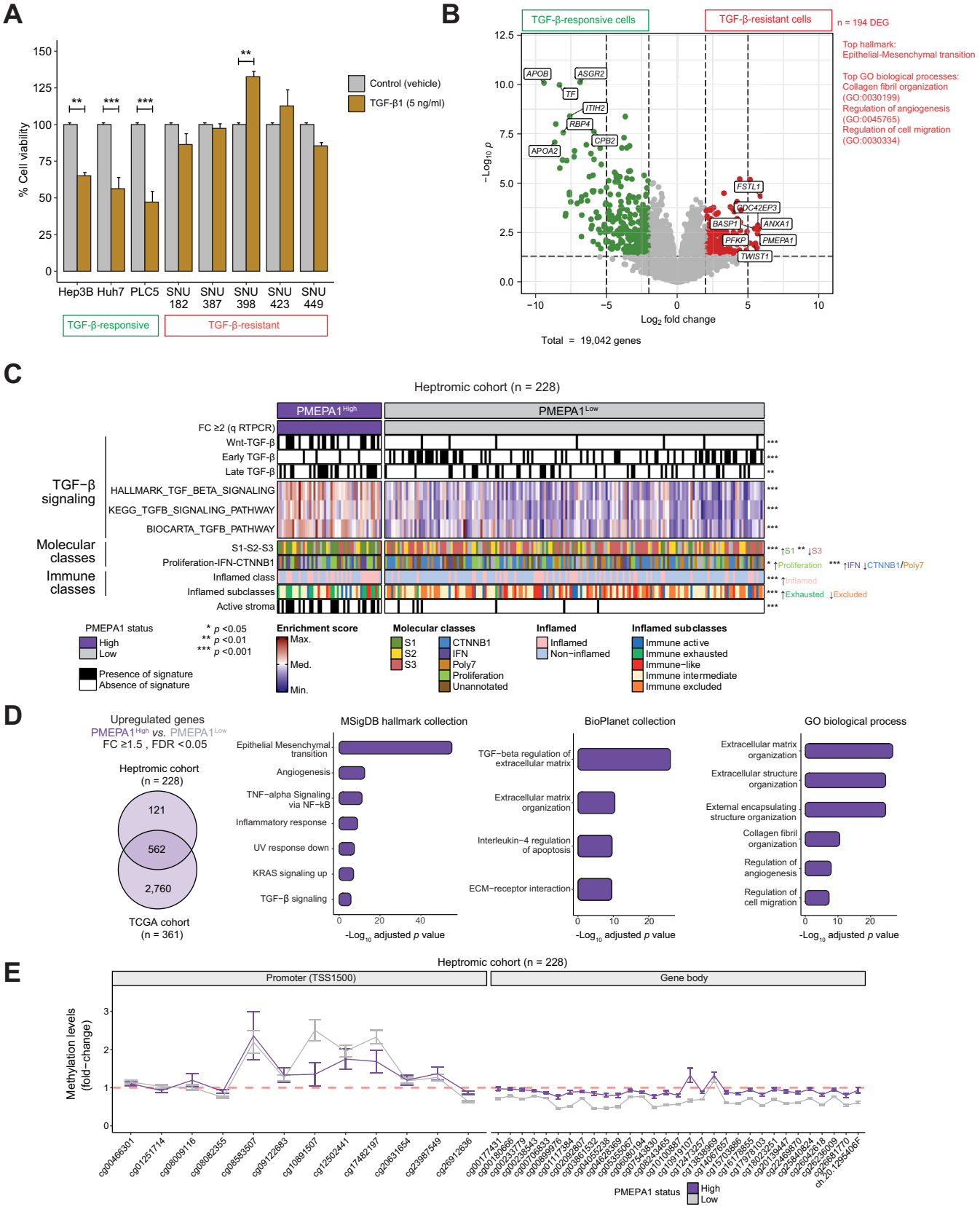

Fig. 1. *PMEPA1* overexpression in human HCC. (A) Cell viability after 3 days of incubation with recombinant human TGF-β1. (B) Volcano plot of genes differentially expressed (FDR <0.05) in HCC cell lines responsive to TGF-β1 stimulation (green) when compared to cells that are resistant to TGF-β1 stimulation (red). Top signalling pathways enriched based on differentially upregulated genes in the TGF-β-resistant condition (n = 194) are depicted in red. (C) Molecular characteristics of *PMEPA1*^{High} human HCCs in the Heptromic cohort (n = 228 patients). Statistical test: Student's *t* test, Wilcoxon rank-sum test or Fisher's exact test, as appropriate. (D) Pathways

PMEPA1 expression in HCC. Interestingly, differential miRNA expression analysis between cell lines with high and low *PMEPA1* levels revealed hsa-miR-192 and hsa-miR-194 to be the most highly upregulated miRNAs in those samples with low *PMEPA1* expression (Fig. S9A,B). Consistently, both hsa-miR-192 and hsa-miR-194 were significantly upregulated in human *PMEPA1*^{Low} samples from both the Heptromic and TCGA datasets when compared to *PMEPA1*^{High} samples (Fig. S10A,B). Of note, *PMEPA1* is a predicted target of both hsa-miR-192-3p and hsa-miR-194-5p according to the TargetScanHuman 7.2 database.[45]

Altogether, *PMEPA1* is overexpressed in 18% of HCCs, and correlates with enhanced TGF-β signalling, increased cellular proliferation, and immune exhaustion. We propose epigenetic deregulation as a potential mechanism of regulation of *PMEPA1* expression.

Exhaustion and poor prognosis features of *PMEPA1*^{High} HCC are driven by TGF-β

We next addressed the role of TGF-β within *PMEPA1*^{High} human tumours. To define TGF-β activation, we used the HCC Wnt-TGF-β gene signature,[17] which presented a strong correlation with both the Hallmark of TGF-β signalling (Fig. S11A) and TGF-β1 expression (Fig. S11B). Overall, this signature classified ∼20% of HCCs as TGF-β-active (n = 123/589). A total of 12% of tumours in the Heptromic cohort (n = 28/228) presented *PMEPA1* overexpression along with TGF-β activation (Fig. 2A). When compared with tumours with *PMEPA1* overexpression but no TGF-β activation, PMEPA1^{High}/TGF-β-activated tumours retained an enrichment in the TGF-β late signature – capturing the TGF-β oncogenic traits[18] – the S1/proliferation HCC molecular subclasses,[6,37] and gene sets capturing cell proliferation, angiogenesis, cell invasion and migration (p <0.05, Fig. 2A). In addition, they were characterized by an active stroma[46] and were primarily classified as immune exhausted[9] (p <0.05, Fig. 2A).

These distinctive features of *PMEPA1*^{High}/TGF-β-activated tumours were neither retained in HCCs with TGF-β activation without *PMEPA1* upregulation, nor in tumours with *PMEPA1* overexpression without TGF-β activation. All these results were validated in the TCGA dataset, as well as in three additional human HCC cohorts (Fig. S12).

Additionally, since *PMEPA1* has been reported to inhibit the androgen receptor (AR) via a negative feedback loop,[47] and AR has been shown to hinder HCC progression,[48] we went on to assess AR protein expression levels in the context of *PMEPA1* overexpression and TGF-β signalling using the TCGA protein array (RPPA) data. We observed a significant decrease in AR protein levels in *PMEPA1*^{High} tumours compared to *PMEPA1*^{Low} HCCs regardless of TGF-β activation status (Fig. 2B), pointing towards a TGF-β-independent role of *PMEPA1* in suppressing androgen response signalling. These results were paralleled when assessing *PMEPA1* and *AR* abundance at the transcriptomic level, both in the Heptromic and TCGA cohorts (Fig. S13).

Finally, since *PMEPA1* has been proposed as a potential prognostic biomarker in other tumour types, we evaluated its association with recurrence in HCC. Importantly, patients belonging to the *PMEPA1*^{High}/TGF-β-activated subgroup displayed significantly higher recurrence rates compared to the rest of the cohort (p = 0.02, Fig. 2C), while this was not the case for the *PMEPA1*^{High} subgroup, including TGF-β-inactivated patients. Importantly, the *PMEPA1*^{High}/TGF-β-activated status retained a significant correlation with higher recurrence rates in the multivariate analysis (Table 1). These results were validated in an independent cohort (Fig. S14, Table S7).

Overall, our analyses revealed the existence of a well-defined subgroup of HCC patients (∼12%) characterized by *PMEPA1* overexpression in the presence of TGF-β signalling activation that specifically display transcriptomic features of immune exhaustion and a more aggressive tumour phenotype, resulting in a significantly worse clinical prognosis. These features were not observed in HCCs characterized by *PMEPA1* overexpression or TGF-β activation alone.

Single-cell RNA sequencing analysis reveals that *PMEPA1* is expressed by both tumoural and TME cells that interact with immune-exhausted T cells

To further explore the immune exhaustion phenotype observed in the human HCC context, we used two scRNAseq datasets comprising 16 and 38 HCCs, respectively.[33,49] Our analyses revealed that *PMEPA1* is not only expressed by tumour cells but also by cells in the stromal compartment (endothelial cells, pericytes and fibroblasts) and immune cells (plasmacytoid dendritic cells) in both scRNAseq cohorts (Fig. 3A,B and Fig. S15A,B). Ingenuity Pathway Analysis of genes upregulated in *PMEPA1*$^{+}$ tumour cells *vs*. *PMEPA1*$^{-}$ tumour cells revealed a significant association with liver proliferation and regeneration (Fig. S16).

To further explore the relationship between *PMEPA1* overexpression and immune exhaustion observed in the human bulk transcriptome, we used CellChat to look for relevant cell-cell communication interactions between immunosuppressive or exhausted T cells and tumour/stromal cell types, which were categorized into *PMEPA1*$^{+}$ and *PMEPA1*$^{-}$ groups. Specifically, in the scRNAseq cohort comprising n = 16 cases, we observed that *PMEPA1*$^{+}$ tumour cells interact with CD8^{+} exhausted T cells, CD4^{+} regulatory T cells and CD4^{+} CXCL13^{+} T cells through the PVR-TIGIT ligand-receptor pair, while this was not observed in *PMEPA1*$^{-}$ tumour cells (p <0.01) (Fig. 3C). In the scRNAseq dataset of 38 HCCs, another ligand-receptor pair involving TIGIT, namely NECTIN2-TIGIT, was significantly enriched in *PMEPA1*$^{+}$ tumour cells (Fig. S17A). Additionally, in both scRNAseq datasets, *PMEPA1*$^{+}$ endothelial cells were shown to interact with

and biological processes enriched based on n = 562 differentially upregulated genes in *PMEPA1*^{High} tumours compared to *PMEPA1*^{Low} tumours in both Heptromic and TCGA cohorts (n = 228 and n = 361 patients, respectively), using Comparative Marker Selection analysis. (E) Methylation array levels in CpGs located within the *PMEPA1* promoter or gene body in *PMEPA1*^{High} (purple) and *PMEPA1*^{Low} (grey) samples in the Heptromic cohort. Values represent the mean β-value in each CpG and bars represent the SD between samples. FC is normalized to 1 (mean expression value in non-tumour liver). DEGs, differentially expressed genes; FC, fold-change; FDR, false discovery rate; GO, gene ontology; HCC, hepatocellular carcinoma; TCGA, The Cancer Genome Atlas; TSS, transcription start site.

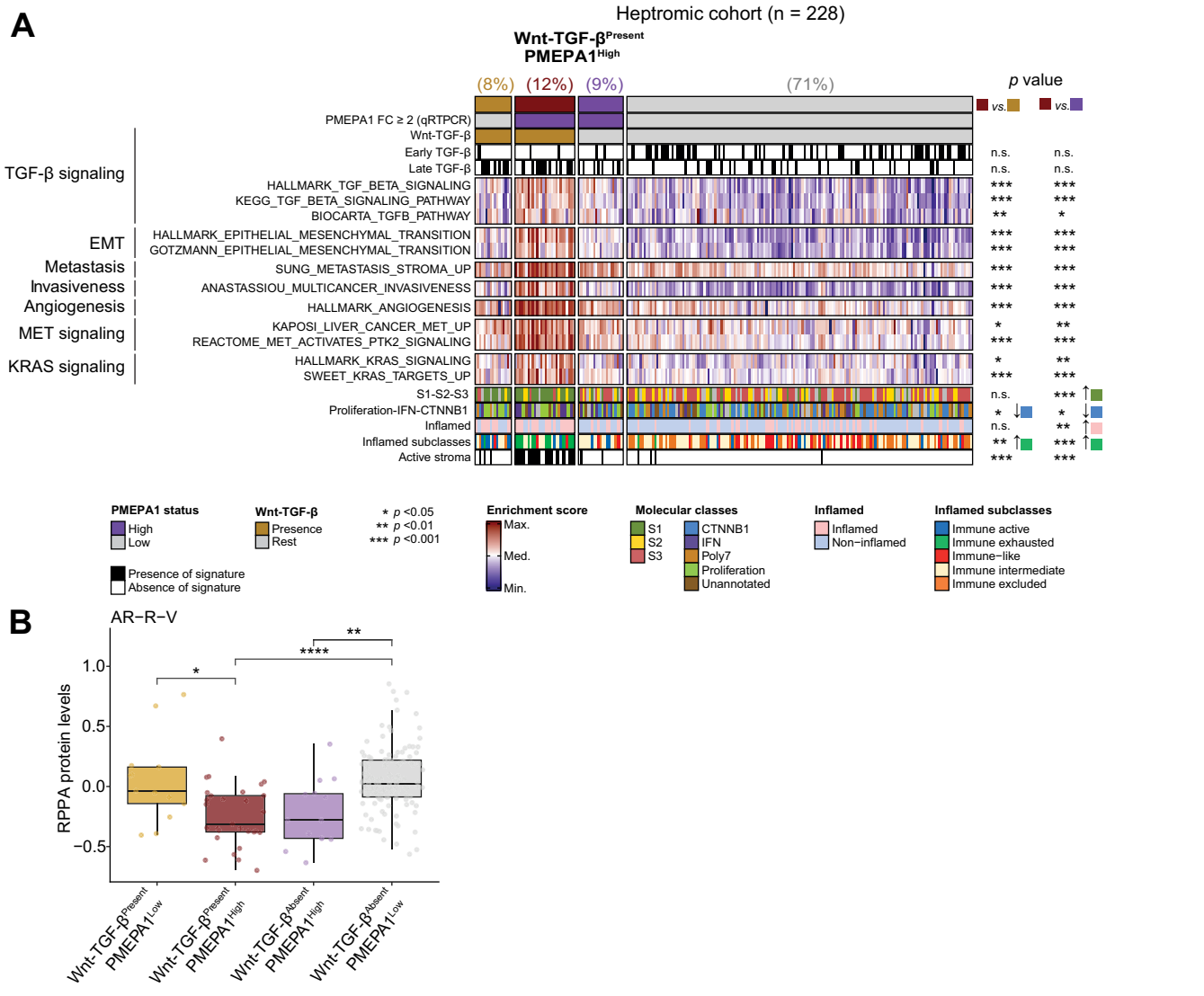

Fig. 2. *PMEPA1* overexpression in the context of Wnt-TGF-β signalling in human HCC. (A) Molecular features of Wnt-TGF-β^{Present}/*PMEPA1*^{High} tumours in the Heptromic cohort when compared to tumours classified as Wnt-TGF-β^{Present}/*PMEPA1*^{High} or Wnt-TGF-β^{Absent}/*PMEPA1*^{High}. Statistical test: Student's *t* test, Wilcoxon rank-sum test or Fisher's exact test, as appropriate. (B) AR protein expression levels assessed by TCGA protein array (RPPA) in samples from the TCGA cohort

Table 1. Univariate and multivariate recurrence rate analyses of patients with HCC (n = 217).

	Univariate analysis			Multivariate analysis (Cox regression)		
Variable	**HR**	**95% CI**	***p* values**	**HR**	**95% CI**	***p* values**
Wnt-TGF-β^{Present} + *PMEPA1*^{High}	1.645	1.061–2.551	0.02	1.902	1.2131–2.984	0.0051
Vascular invasion	1.576	1.128–2.201	0.007			
BCLC stage B or C	1.731	1.068–2.807	0.02			
Multinodularity	2.05	1.445–2.921	0.00004	1.916	1.2957–2.833	0.0011
AFP levels (>100 mg/dl)	1.66	1.149–2.406	0.007			
Satellites	1.603	1.12–2.296	0.009	1.647	1.1388–2.383	0.0081

AFP, alpha-fetoprotein; BCLC, Barcelona Clinic Liver Cancer; HCC, hepatocellular carcinoma; HR, hazard ratio.

CD8$^+$ exhausted T cells through the LGALS9-HAVCR2 ligand-receptor pair, an observation that was not made for *PMEPA1*$^-$ endothelial cells (Fig. S17B). Given the role of TIGIT and HAVCR2 (TIM-3) as T cell exhaustion-associated checkpoint molecules, these findings underscore the association between *PMEPA1* expression and immune exhaustion.

PMEPA1 and *MYC* overexpression promote HCC development in a genetically engineered mouse model

Since *PMEPA1* has been reported to act as an oncogene in other tumour types, we assessed its function in HCC using *in vitro* and *in vivo* models. Firstly, we engineered HCC cells with low baseline *PMEPA1* mRNA levels and responsiveness to the cytostatic effects of TGF-β1 (Fig. S1A and Fig. 1A) (Hep3B, PLC5 and Huh7) to stably overexpress *PMEPA1* (Fig. S18A), with and without TGF-β1 stimulation. Proliferation and viability assays revealed that *PMEPA1* did not show a significant oncogenic effect (Fig. S18B-D). Thus, we hypothesized that the TME might influence the ability of *PMEPA1* to exert its oncogenic function. To test this hypothesis, we generated a genetically engineered mosaic mouse model (GEMM) overexpressing both *PMEPA1* and *MYC* in the liver, in the context of an intact TME. As a control arm, we used a GEMM that overexpressed *MYC* alone (Fig. 4A), which is known to be insufficient to trigger HCC development.[50] Strikingly, 60% of mice injected with *MYC;PMEPA1* developed tumours (n = 9/15, Fig. 4B,C) resulting in a significantly higher liver to body weight ratio compared to *MYC* controls (p <0.001; Fig. S19). Consequently, we observed a significant reduction in survival compared to *MYC* controls (p = 0.014, Fig. 4C). HCC and PMEPA1 protein expression levels were confirmed at the pathological level (Fig. 4D).

Consistent with our results using the human HCC cohorts, transcriptomic analyses of the *MYC;PMEPA1* tumours (n = 4) revealed that they were significantly enriched in gene signatures recapitulating TGF-β signalling when compared to *MYC-luc;CTNNB1* tumours (n = 7) and healthy liver tissue (n = 6) (Fig. 5A). On the other hand, *MYC;PMEPA1* tumours were transcriptionally resemblant to *MYC-lucOS;p53* tumours, which include the highly immunogenic version of luciferase (*MYC-lucOS*), associated with high oncogenicity, aggressiveness and poor prognosis (Fig. S20).[36,50] In addition, a decrease in Wnt/β-catenin signalling, as well as negative glutamine synthetase immunohistochemical staining (Fig. S21), was observed in tumours from *MYC;PMEPA1* mice when compared with the *MYC-luc;CTNNB1* model. Further analyses also unveiled that *MYC;PMEPA1* tumours were enriched in the proliferation subclass (S1/S2,[6] Proliferation class[37]) and other proliferation-related signatures (*e.g.* KRAS and MYC) (Fig. 5A), as well as hypoxia and invasiveness gene sets. These results suggest that the *MYC;PMEPA1* model recapitulates the human *PMEPA1*-^{High}/TGF-β-activated scenario.

Additionally, in line with our results in *PMEPA1*^{High} human HCC samples (Fig. 2B), *MYC;PMEPA1* tumours presented a reduced expression of androgen response signatures compared to both *MYC-luc;CTNNB1* tumours and healthy liver tissue (Fig. 5A). This was supported by a significantly reduced expression of *AR* compared to healthy liver tissue (Fig. 5B).

At the pathological level, *MYC;PMEPA1* tumours were "moderately" and "well" differentiated, while all the *MYC-luc;CTNNB1* tumours were "well" differentiated (Fig. 5C), compared to other previously reported GEMMs of HCC (*MYC-luc;CTNNB1* and *MYC-lucOS;p53*). No significant differences were identified between models in terms of immune infiltrate or necrosis percentage (Fig. S22).

In sum, these *in vivo* data demonstrate the oncogenic role of *PMEPA1* in the context of TGF-β signalling in HCC.

Discussion

The role of the TGF-β pathway in HCC has been thoroughly studied over the years, but there is still no clear consensus on what causes the pathway to exert its pro-tumoural *vs*. tumour-suppressive effects.[51,52] Herein, we investigated the role of *PMEPA1* in the context of TGF-β signalling using bulk transcriptomic data of >500 human HCC samples, and found that the combined overexpression of *PMEPA1* and TGF-β pathway activation (12% of HCCs) is associated with an immune-exhausted TME, aggressive tumours and poor clinical outcomes. Importantly, scRNAseq analysis revealed that *PMEPA1* is expressed not only by tumour cells but also by stromal types present in the HCC TME. *In vivo*, we demonstrated that liver-specific *PMEPA1* overexpression promotes hepatocarcinogenesis, highlighting the oncogenic capacity of *PMEPA1* in HCC for the first time.

PMEPA1 overexpression has been reported in a wide variety of cancers, including ovarian, breast, renal and colorectal tumours.[53–56] Herein, we evaluated *PMEPA1* levels in seven independent HCC cohorts and found it to be overexpressed in 18% of cases. *PMEPA1* expression has been previously

according to their Wnt-TGF-β/*PMEPA1* status. Statistical test: Wilcoxon rank-sum test. Adjusted p values, computed using the Benjamini-Hochberg method, are depicted. (C) Kaplan-Meier estimates of recurrence in patients with HCC from the Heptromic cohort based on *PMEPA1*^{High} status (left) or Wnt-TGF-β^{Present}/*PMEPA1*^{High} status (right). Statistical test: log-rank test. EMT, epithelial-mesenchymal transition; HCC, hepatocellular carcinoma; TCGA, The Cancer Genome Atlas.

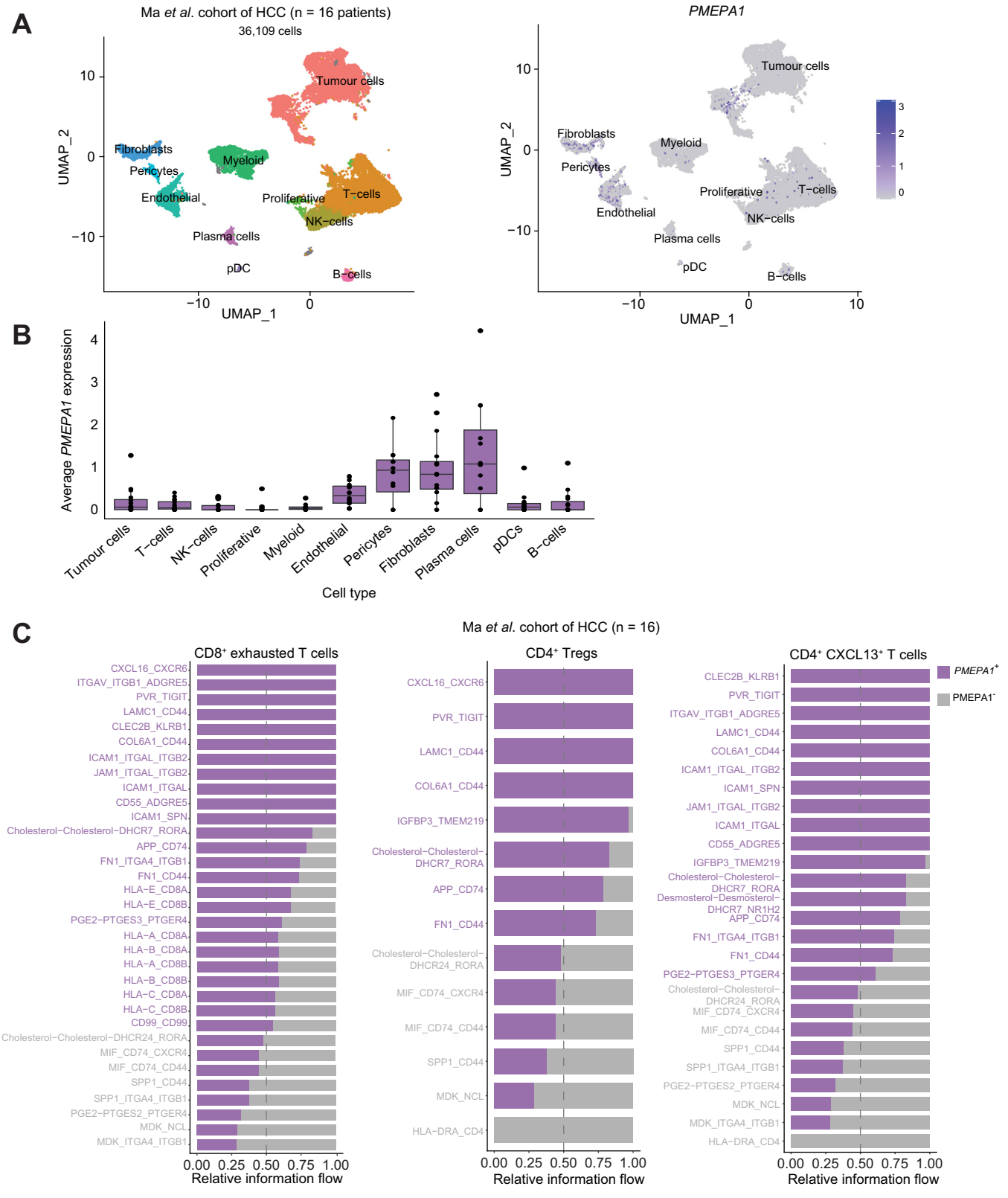

Fig. 3. Single-cell RNA sequencing assessment of *PMEPA1* expression in HCC. (A) UMAP projection of the cell types present in the scRNA-seq dataset comprising 16 patients with HCC (left panel) and with the overlaid *PMEPA1* expression level (right panel). (B) Boxplot representation of the average *PMEPA1* expression in each cell type of the TME. (C) Bar plot depicting the relative information flow for each ligand-receptor pair between tumour cells (source), coloured according to *PMEPA1*$^{+}$ status, and CD8^{+} exhausted T cells, CD4^{+} Tregs, and CD4^{+} CXCL13^{+} T cells (target cells) in a scRNAseq cohort of 16 patients with HCC. Ligand-receptor pairs in blue text present a significantly higher information flow in *PMEPA1*$^{+}$ tumour cells, while beige text denotes significance in their *PMEPA1*$^{-}$ counterparts (p <0.01). p values were calculated using a two-sided Wilcoxon test. HCC, hepatocellular carcinoma; pDCs, plasmacytoid dendritic cells; scRNAseq, single-cell RNA sequencing; TME, tumour microenvironment; Tregs, regulatory T cells; UMAP, uniform manifold approximation and projection.

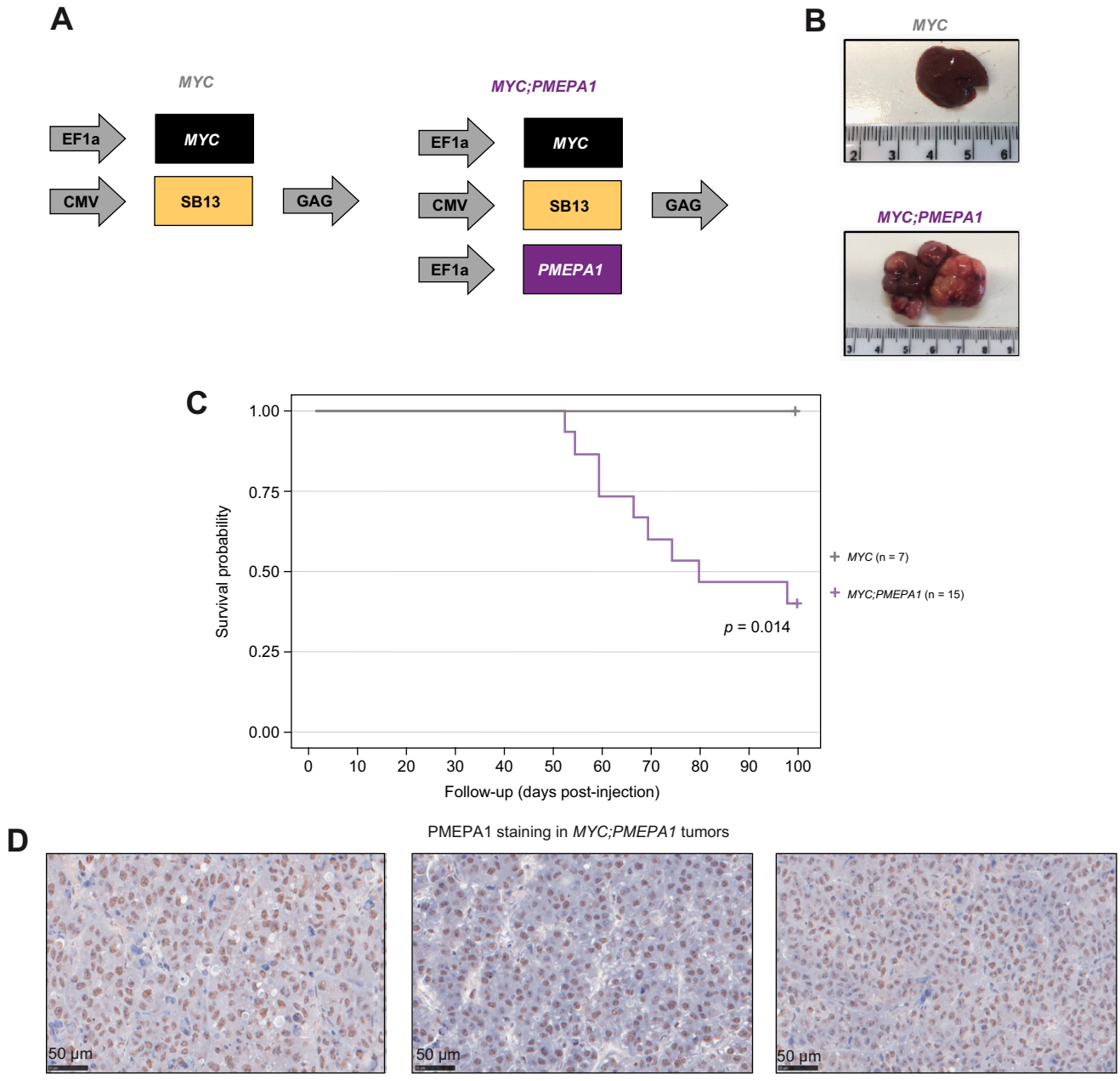

Fig. 4. *PMEPA1* promotes HCC development *in vivo*. (A) Schematic of vectors injected into the mice of the two experimental arms. (B) Representative images of livers from *MYC* alone or *MYC;PMEPA1* models at study endpoint. (C) Median survival of *MYC* and *MYC;PMEPA1* animals. Statistical test: log-rank test. Number of mice per group is also shown. (D) Representative images of PMEPA1 protein levels in *MYC;PMEPA1* and *MYC-luc;CTNNB1* murine tumours (20X; 100 mm). HCC, hepatocellular carcinoma.

reported to be controlled by epigenetic mechanisms.[19,41,44] Moreover, hypomethylation of the gene body has been previously shown to correlate with a low transcription rate of commonly upregulated genes in cancer.[42] Accordingly, our data suggest that a reduction in *PMEPA1* expression is associated with hypomethylation within the *PMEPA1* gene body.

Our transcriptomic integrative analysis revealed that HCCs with both overexpression of *PMEPA1* and activation of the TGF-β pathway display a more aggressive phenotype than tumours with only *PMEPA1* overexpression or TGF-β activation, as evidenced by an enrichment of proliferation, invasiveness, and migration features. Tumours with *PMEPA1* overexpression and absence of Wnt-TGF-β signalling activation also retained features related to HCC aggressiveness. Importantly, the immune-exhausted features of *PMEPA1*^{High}/TGF-β-active tumours were exclusive to this condition. *PMEPA1* levels and features of immune exhaustion have previously been linked not only in HCC but in other tumour types; however, no further insights into this association have been reported.[57] Our scRNAseq analysis further shed light on the

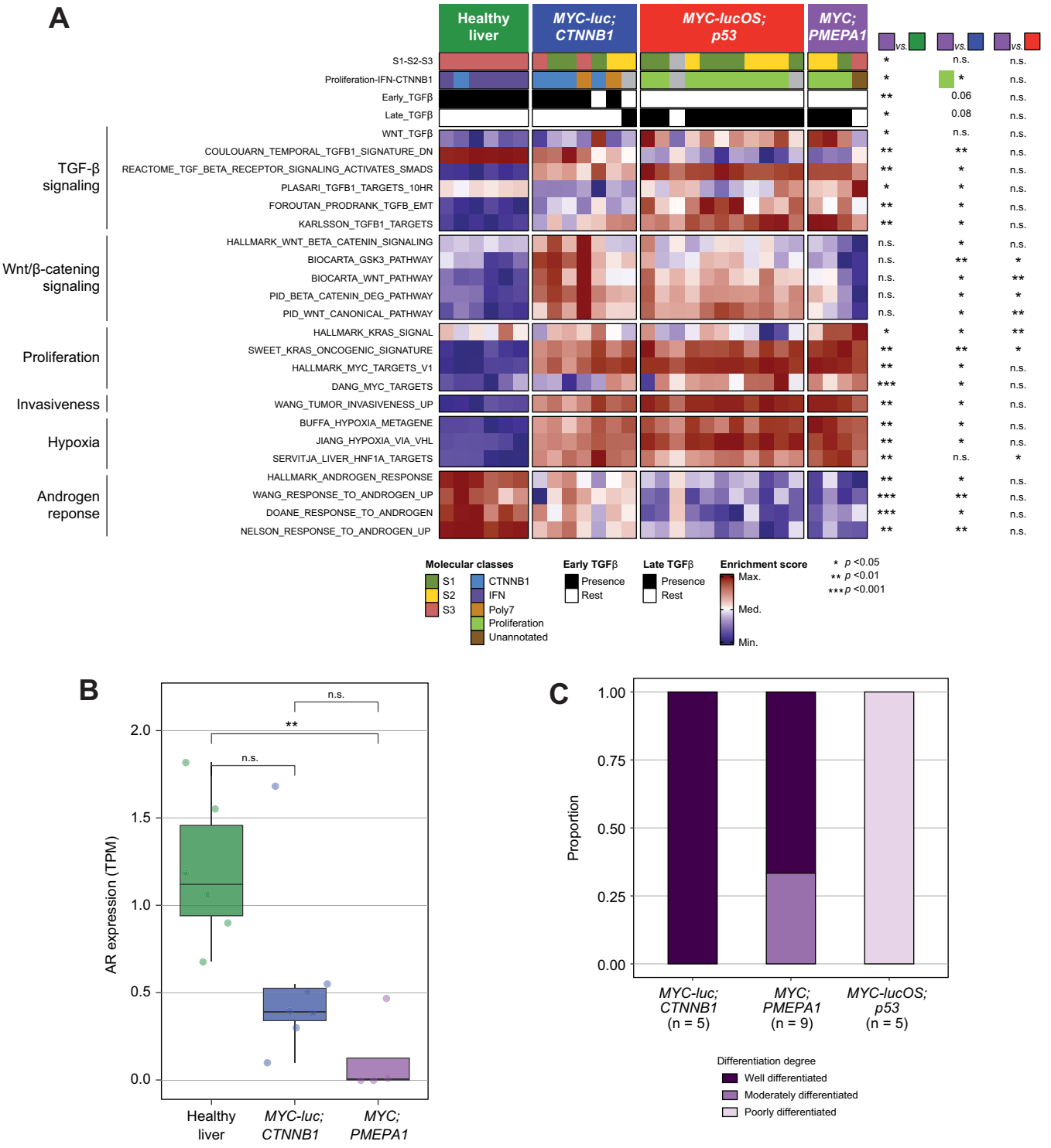

Fig. 5. Transcriptomic and histopathological characterization of *MYC;PMEPA1* tumours. (A) Heatmap representing molecular features and signalling pathways of *MYC;PMEPA1* tumours in comparison with *MYC-luc;CTNNB1* and *MYC-lucOS;p53* tumours and healthy liver tissue. Statistical test: Student's *t* test, Wilcoxon rank-sum test or Fisher's exact test, as appropriate. (B) Boxplots depicting AR expression levels (TPM) in healthy liver tissue, *MYC-luc;CTNNB1* and *MYC;PMEPA1* tumours. Statistical test: Wilcoxon rank-sum test. Adjusted *p* values, computed using the Benjamini-Hochberg method, are depicted. (C) Barplot depicting the proportion of each tumour differentiation degree category in *MYC;PMEPA1*, *MYC-luc;CTNNB1* and *MYC-lucOS;p53* GEMMs. GEMMs, genetically engineered mosaic mouse models; TPM, transcripts per million.

association between *PMEPA1* overexpression – in tumour and stromal cells – and immune exhaustion in HCC. Specifically, we observed that *PMEPA1*-expressing tumour and endothelial cells, but not their *PMEPA1*$^{-}$ counterparts, interact with exhausted T cells through ligand-receptor pairs involving key checkpoint molecules such as TIGIT and TIM-3.

Given the relevance of the stromal compartment towards *PMEPA1* function in HCC, we used a well-established murine model of HCC to evaluate the role of *PMEPA1* in the context of an intact TME. Specifically, we used a model where overexpression of *MYC* alone, an oncogene that is amplified in HCC,[58] needs a second hit for tumour development. A major finding of the present study was that *PMEPA1* and *MYC* overexpression in the liver leads to tumour development, describing for the first time the oncogenic capacity of *PMEPA1* in HCC. Of note, this gene has previously been shown to promote tumour growth in ovarian cancer xenograft models,[56] and has been drugged and identified as a potential therapeutic target in triple negative breast cancer.[59]

Transcriptomic analyses revealed an underlying activation of TGF-β signalling in the *MYC;PMEPA1* model when compared to control tumours generated by overexpression of *MYC* and *CTNNB1* and to murine liver samples, which confirms that our model recapitulates many of the traits that were observed in human HCC samples. In this line, data from both human and murine HCCs overexpressing *PMEPA1* suggest that in addition to promoting TGF-β oncogenic signalling in HCC, *PMEPA1* might also play a role in suppressing *AR* levels and androgen response signalling, as previously described in prostate cancer cells.[41] In the HCC context, AR signalling has been shown to suppress metastasis in advanced stages,[60] thus suggesting that *PMEPA1*-mediated repression of *AR* could also contribute to its oncogenic effects.

In conclusion, our study elucidated the role of *PMEPA1* in human HCC, showing that *PMEPA1* overexpression is associated with tumour aggressiveness and immune exhaustion when TGF-β activation is also present. Additionally, scRNAseq revealed that *PMEPA1* plays a role in the TME and impacts the interaction between tumour cells and exhausted T cells in HCC. Finally, we demonstrated the oncogenic capacity of *PMEPA1* in HCC by using a GEMM, which was linked to TGF-β signalling and a reduced androgen response. This study identifies *PMEPA1* as a novel oncogene whose activity is linked to the tumour-promoting effects of TGF-β in HCC.

Affiliations

[1]*Liver Cancer Translational Research Group, Institut d'Investigacions Biomèdiques August Pi i Sunyer (IDIBAPS), Hospital Clínic, Universitat de Barcelona, Barcelona, Catalonia, Spain;* [2]*Mount Sinai Liver Cancer Program (Divisions of Liver Diseases, Department of Hematology/Oncology, Department of Medicine, Department of Pathology), Tisch Cancer Institute, Icahn School of Medicine at Mount Sinai, New York, USA;* [3]*Pathology Department & Molecular Biology CORE, Biomedical Diagnostic Center, Barcelona Hospital Clínic, University of Barcelona, Barcelona, Catalonia, Spain;* [4]*Digestive Oncology, Department of Gastroenterology, University Hospitals Leuven, Leuven, Belgium;* [5]*Laboratory of Clinical Digestive Oncology, Department of Oncology, KU Leuven, Leuven, Belgium;* [6]*Laboratory for Translational Genetics, Department of Human Genetics, VIB and KU Leuven, Leuven, Belgium;* [7]*VIB Centre for Cancer Biology, Leuven, Belgium;* [8]*Institució Catalana de Recerca i Estudis Avançats, Barcelona, Catalonia, Spain*

Abbreviations

AR, androgen receptor; EMT, epithelial-mesenchymal transition; ECM, extracellular matrix; GEMM, genetically engineered mosaic mouse model; HCC, hepatocellular carcinoma; PMEPA1, prostate transmembrane protein androgen induced 1; scRNAseq, single-cell RNA sequencing; TCGA, The Cancer Genome Atlas; TGF-β, transforming growth factor-β; TME, tumour microenvironment.

Financial support

MPG was supported by a pre-doctoral grant from the Spanish National Health Institute (MICINN, PRE2020-094716) and a mobility grant from "Fundació Universitària Agustí Pedro i Pons". CAO was supported by a Fulbright fellowship and a "laCaixa" INPhINIT Fellowship (LCF/BQ/IN17/11620024). AM was supported by Generalitat de Catalunya with a FI-SDUR fellowship (2021 FISDU 00338) from AGAUR. REF was supported by a predoctoral grant from the Spanish National Health Institute (MCINN; BES-2017-081286) and a mobility grant from "Fundació Universitària Agustí Pedro i Pons". MBV was supported by Asociación Española del Estudio del Hígado (AEEH), Fundación Ramón Areces, and Cholangiocarcinoma Foundation. MRG was supported by Fundación Alfonso Martín Escudero Fellowship. SC was supported by a strategic basic research fellowship from Research Foundation— Flanders (FWO; 1S95221N) and a post-doctoral fellowship from the Belgian American Educational Foundation (BAEF). JP was supported by a PERIS ICT-Suport grant from the "Departament de Salut de la Generalitat de Catalunya" (SLT017/20/000206). IK was supported by Asociación Española del Estudio del Hígado (AEEH). JAF was supported by a doctoral training grant from the University of Barcelona (PREDOCS-UB 2020) and by the "Societat Catalana de Digestologia" mobility grant. KEL was supported by T32 5T32CA078207-22, 2T32CA078207-21, and 5T32AI078892-12. DS was supported by grants from the Department of Defense (RA220126), National Health Institute (NIH 75N91022R00006) and American Cancer Society Research Scholar Grant RSG-23-1151048-01. AL was supported by Damon Runyon-Rachleff Innovation Award (DR52-18) and R37 Merit Award (R37CA230636), and Icahn School of Medicine at Mount Sinai. The Tisch Cancer Institute and related research facilities are supported by P30 CA196521. RP was supported by the Fundació de Recerca Clínic Barcelona - IDIBAPS and by a grant from the Spanish National Health Institute (MICINN, PID2022-139365OB-I00). JML was supported by grants from the European Commission (Horizon Europe-Mission Cancer, THRIVE, Ref. 101136622), by an Accelerator Award from Cancer Research UK, Fondazione per la Ricerca sul Cancro (AIRC) and Fundación Científica de la Asociación Española Contra el Cáncer (FAECC) (HUNTER, Ref. C9380/A26813), by the NIH (R01-CA273932-01, R01DK56621 and R01DK128289), the Samuel Waxman Cancer Research Foundation, the Spanish National Health Institute (Project PID2022-139365OB-I00, funded by MICIU/AEI/10.13039/501100011033 and FEDER); the Asociación Española Contra el Cáncer (Proyectos Generales: PRYGN223117LLOV; Reto AECC 70% Supervivencia: RETOS245779LLOV), the Generalitat de Catalunya (AGAUR, 2021-SGR 01347), the "la Caixa" Banking Foundation and the Acadèmia de Ciències Mèdiques i de la Salut de Catalunya i Balears.

Conflict of interest

DL is a consultant for DROIA Investment Board, Montis Biosciences, received Grant/Research support from AstraZeneca, MSD, and Bristol-Myers-Squibb, and honoraria from AstraZeneca, MSD, Bristol-Myers-Squibb, and Hedera Dx. JD received consulting fees and/or speaker honoraria from Amgen, AstraZeneca, Bayer, BMS, Eisai, Need Inc., Ipsen, Lilly, MediMix, Merck, MSD, Novartis, Roche and Servier. JML is receiving research support from Eisai Inc, Boehringer-Ingelheim, Bayer Pharmaceuticals, Bristol-Myers Squibb and Ipsen, and consulting fees from Eisai Inc, Merck, Roche, Genentech, AstraZeneca, Bayer Pharmaceuticals, Bristol-Myers Squibb, Chugai, Abbvie, Eli Lilly, Ipsen, Sanofi, Moderna, Glycotest, Exelixis, Sagimet, Boston Scientific and Bluejay.

Please refer to the accompanying ICMJE disclosure forms for further details.

Authors' contributions

RP and JML designed and supervised the study, with help from AL and DS. MPG, CAO, AM, REF, MBV, MRG, CM, SC, JP, EFM, EM, MTM, JAF, KEL, ST and RP performed experiments/analysis. MPG, CAO, AM, REF, MBV, IK, AGO, DL, JD, DS, AL, RP and JML provided scientific input. The manuscript was written by MPG, CAO and RP under supervision of JML. All authors were involved in the critical revision of the manuscript.

Data availability statement

Data are available in a public, open access repository. The RNA sequencing data from the *MYC;PMEPA1* murine model have been deposited at GEO with accession number GSE274750.

Acknowledgements

Concerning the single-cell RNAseq cohort comprising 38 human HCCs: The computational resources and services used in this work were partly provided by the Flemish Supercomputer Center (VSC), funded by the Research Foundation – Flanders (FWO) and the Flemish Government department EWI. This study was supported by the 'Stichting Tegen Kanker' (FAF-C/2018/1297) grant. This study has been developed in part in the Centre Esther Koplowitz from IDIBAPS/CERCA Programme/Generalitat de Catalunya. Genomic analyses were run at the Genomics Core Facility from the Icahn School of Medicine at Mount Sinai. This work was supported in part through the computational and data resources and staff expertise provided by Scientific Computing and Data at the Icahn School of Medicine at Mount Sinai and supported by the Clinical and Translational Science Awards (CTSA) grant UL1TR004419 from the National Center for Advancing Translational Sciences. Research reported in this publication was also supported by the Office of Research Infrastructure of the National Institutes of Health under award number S10OD026880 and S10OD030463. The content is solely the responsibility of the authors and does not necessarily represent the official views of the National Institutes of Health. The Graphical Abstract was created with BioRender.com.

Supplementary data

Supplementary data to this article can be found online at https://doi.org/10.1016/j.jhepr.2024.101212.

References

Author names in bold designate shared co-first authorship

[1] Sung H, Ferlay J, Siegel RL, et al. Global cancer statistics 2020: GLOBOCAN estimates of incidence and mortality worldwide for 36 cancers in 185 countries. CA Cancer J Clin 2021;71:209–249.
[2] Llovet JM, Kelley RK, Villanueva A, et al. Hepatocellular carcinoma. Nat Rev Dis Primers 2021;7:6.
[3] **Schulze K**, **Imbeaud S**, **Letouzé E**, et al. Exome sequencing of hepatocellular carcinomas identifies new mutational signatures and potential therapeutic targets. Nat Genet 2015;47:505–511.
[4] Llovet JM, Pinyol R, Kelley RK, et al. Molecular pathogenesis and systemic therapies for hepatocellular carcinoma. Nat Cancer 2022;3:386–401.
[5] Llovet JM, Castet F, Heikenwalder M, et al. Immunotherapies for hepatocellular carcinoma. Nat Rev Clin Oncol 2022;19:151–172.
[6] Hoshida Y, Nijman SMBS, Kobayashi M, et al. Integrative transcriptome analysis reveals common molecular subclasses of human hepatocellular carcinoma. Cancer Res 2009;69:7385–7392.
[7] Lachenmayer A, Alsinet C, Savic R, et al. Wnt pathway activation in two molecular classes of hepatocellular carcinoma and experimental modulation by sorafenib. Clin Cancer Res 2012;18:4997–5007.
[8] **Montironi C**, **Castet F**, **Haber PK**, et al. Inflamed and non-inflamed classes of HCC: a revised immunogenomic classification. Gut 2023;72:129–140.
[9] Sia D, Jiao Y, Martinez-Quetglas I, et al. Identification of an immune-specific class of hepatocellular carcinoma, based on molecular features. Gastroenterology 2017;153:812–826.
[10] Chen J, Zaidi S, Rao S, et al. Analysis of genomes and transcriptomes of hepatocellular carcinomas identifies mutations and gene expression changes in the transforming growth factor-β pathway. Gastroenterology 2018;154:195–210.
[11] Gonzalez-Sanchez E, Vaquero J, Férnandez-Barrena MG, et al. The TGF-β pathway: a pharmacological target in hepatocellular carcinoma? Cancers (Basel) 2021;13:3248.
[12] Batlle E, Massagué J. Transforming growth factor-β signaling in immunity and cancer. Immunity 2019;50:924–940.
[13] Seoane J, Gomis RR. TGF- family signaling 675 in tumor suppression and cancer progression. Cold Spring Harb Perspect Biol 2017;9:a022277.
[14] David CJ, Massagué J. Contextual determinants of TGFβ action in development, immunity and cancer. Nat Rev Mol Cell Biol 2018;19:419–435.
[15] Mariathasan S, Turley SJ, Nickles D, et al. TGFβ attenuates tumour response to PD-L1 blockade by contributing to exclusion of T cells. Nature 2018;554:544–548.
[16] Tauriello DVF, Sancho E, Batlle E. Overcoming TGFβ-mediated immune evasion in cancer. Nat Rev Cancer 2022;22:25–44.
[17] Lachenmayer A, Alsinet C, Savic R, et al. Wnt pathway activation in two molecular classes of hepatocellular carcinoma and experimental modulation by sorafenib. Clin Cancer Res 2012;18:4997–5007.
[18] Coulouarn C, Factor VM, Thorgeirsson SS. Transforming growth factor-β gene expression signature in mouse hepatocytes predicts clinical outcome in human cancer. Hepatology 2008;47:2059–2067.
[19] Fournier PGJ, Juárez P, Jiang G, et al. The TGF-β signaling regulator PMEPA1 suppresses prostate cancer metastases to bone. Cancer Cell 2015;27:809–821.
[20] Singha PK, Pandeswara S, Geng H, et al. TGF-β induced TMEPAI/PMEPA1 inhibits canonical Smad signaling through R-Smad sequestration and promotes non-canonical PI3K/Akt signaling by reducing PTEN in triple negative breast cancer. Genes Cancer 2014;5:320–336.
[21] Singha PK, Pandeswara S, Geng H, et al. Increased Smad3 and reduced Smad2 levels mediate the functional switch of TGF-β from growth suppressor to growth and metastasis promoter through TMEPAI/PMEPA1 in triple negative breast cancer. Genes Cancer 2019;10:134–149.
[22] Zhang L, Wang X, Lai C, et al. PMEPA1 induces EMT via a non canonical TGF-β signalling in colorectal cancer. J Cell Mol Med 2019;23:3603–3615.
[23] Wang H, Wang P, Xu M, et al. Distinct functions of transforming growth factor-β signaling in c-MYC driven hepatocellular carcinoma initiation and progression. Cell Death Dis 2021;12:200.
[24] Villanueva A, Portela A, Sayols S, et al. DNA methylation-based prognosis and epidrivers in hepatocellular carcinoma. Hepatology 2015;61:1945–1956.
[25] Makowska Z, Boldanova T, Adametz D, et al. Gene expression analysis of biopsy samples reveals critical limitations of transcriptome-based molecular classifications of hepatocellular carcinoma. J Pathol Clin Res 2016;2:80–92.
[26] Roessler S, Jia H-L, Budhu A, et al. A unique metastasis gene signature enables prediction of tumor relapse in early-stage hepatocellular carcinoma patients. Cancer Res 2010;70:10202–10212.
[27] Roessler S, Long EL, Budhu A, et al. Integrative genomic identification of genes on 8p associated with hepatocellular carcinoma progression and patient survival. Gastroenterology 2012;142:957–966.e12.
[28] Wang H-W, Hsieh T-H, Huang S-Y, et al. Forfeited hepatogenesis program and increased embryonic stem cell traits in young hepatocellular carcinoma (HCC) comparing to elderly HCC. BMC Genomics 2013;14:736.
[29] Kim JH, Sohn BH, Lee H-S, et al. Genomic predictors for recurrence patterns of hepatocellular carcinoma: model derivation and validation. Plos Med 2014;11:e1001770.
[30] **Bassaganyas L**, **Pinyol R**, **Esteban-Fabró R**, et al. Copy-number alteration burden differentially impacts immune profiles and molecular features of hepatocellular carcinoma. Clin Cancer Res 2020;26:6350–6361.
[31] Li T, Fu J, Zeng Z, et al. TIMER2.0 for analysis of tumor infiltrating immune cells. Nucleic Acids Res 2020;48:W509–W514.
[32] Kuleshov MV, Jones MR, Rouillard AD, et al. Enrichr: a comprehensive gene set enrichment analysis web server 2016 update. Nucleic Acids Res 2016;44:W90–W97.
[33] Cappuyns S, Philips G, Vandecaveye V, et al. PD-1- CD45RA+ effector-memory CD8 T cells and CXCL10+ macrophages are associated with response to atezolizumab plus bevacizumab in advanced hepatocellular carcinoma. Nat Commun 2023;14:7825.
[34] Korsunsky I, Millard N, Fan J, et al. Fast, sensitive and accurate integration of single-cell data with Harmony. Nat Methods 2019;16(12):1289–1296.
[35] Jin S, Guerrero-Juarez CF, Zhang L, et al. Inference and analysis of cell-cell communication using CellChat. Nat Commun 2021;12:1088.
[36] Molina-Sánchez P, Ruiz de Galarreta M, Yao MA, et al. Cooperation between distinct cancer driver genes underlies intertumor heterogeneity in hepatocellular carcinoma. Gastroenterology 2020;159:2203–2220.e14.
[37] Chiang DY, Villanueva A, Hoshida Y, et al. Focal gains of VEGFA and molecular classification of hepatocellular carcinoma. Cancer Res 2008;68:6779–6788.
[38] Moffitt RA, Marayati R, Flate EL, et al. Virtual microdissection identifies distinct tumor- and stroma-specific subtypes of pancreatic ductal adenocarcinoma. Nat Genet 2015;47:1168–1178.
[39] Calon A, Espinet E, Palomo-Ponce S, et al. Dependency of colorectal cancer on a TGF-β-driven program in stromal cells for metastasis initiation. Cancer Cell 2012;22:571–584.
[40] Amalia R, Abdelaziz M, Puteri MU, et al. TMEPAI/PMEPA1 inhibits Wnt signaling by regulating β-catenin stability and nuclear accumulation in triple negative breast cancer cells. Cell Signal 2019;59:24–33.
[41] Sharad S, Ravindranath L, Haffner MC, et al. Methylation of the *PMEPA1* gene, a negative regulator of the androgen receptor in prostate cancer. Epigenetics 2014;9:918–927.

[42] Yang X, Han H, De Carvalho DD, et al. Gene body methylation can alter gene expression and is a therapeutic target in cancer. Cancer Cell 2014;26:577–590.
[43] Mendizabal I, Zeng J, Keller TE, Yi SV. Body-hypomethylated human genes harbor extensive intragenic transcriptional activity and are prone to cancer associated dysregulation. Nucleic Acids Res 2017:gkx020.
[44] Feng S, Zhu X, Fan B, et al. miR-19a-3p targets PMEPA1 and induces prostate cancer cell proliferation, migration and invasion. Mol Med Rep 2016;13:4030–4038.
[45] **McGeary SE**, **Lin KS**, Shi CY, et al. The biochemical basis of microRNA targeting efficacy. Science 2019;20(366):eaav1741. 6472.
[46] Murray CJL, Vos T, Lozano R, et al. Disability-adjusted life years (DALYs) for 291 diseases and injuries in 21 regions, 1990-2010: a systematic analysis for the Global Burden of Disease Study 2010. The Lancet 2012;380:2197–2223.
[47] Li H, Xu LL, Masuda K, et al. A feedback loop between the androgen receptor and a NEDD4-binding protein, PMEPA1, in prostate cancer cells. J Biol Chem 2008;283:28988–28995.
[48] Ouyang X, Feng L, Liu G, et al. Androgen receptor (AR) decreases HCC cells migration and invasion via miR-325/ACP5 signaling. J Cancer 2021;12:1915–1925.
[49] Ma L, Wang L, Khatib SA, et al. Single cell atlas of tumor cell evolution in response to therapy in hepatocellular carcinoma and intrahepatic cholangiocarcinoma. J Hepatol 2021;75:1397–1408.
[50] Ruiz de Galarreta M, Bresnahan E, Molina-Sánchez P, et al. β-Catenin activation promotes immune escape and resistance to anti–PD-1 therapy in hepatocellular carcinoma. 811 Cancer Discov 2019;9:1124–1141.
[51] Dituri F, Mancarella S, Cigliano A, et al. TGF-β as multifaceted orchestrator in HCC progression: signaling, EMT, immune microenvironment, and novel therapeutic perspectives. Semin Liver Dis 2019;39 :53–69.
[52] Mu X, Lin S, Yang J, et al. TGF-β signaling is often attenuated during hepatotumorigenesis, but is retained for the malignancy of hepatocellular carcinoma cells. PLoS One 2013;8:e63436.
[53] Rae FK, Hooper JD, Nicol DL, Clements JA. Characterization of a novel gene, STAG1/PMEPA1, upregulated in renal cell carcinoma and other solid tumors. Mol Carcinog 2001;32:44–53.
[54] Giannini G, Ambrosini MI, Di Marcotullio L, et al. EGF- and cell-cycle-regulatedSTAG1/PMEPA1/ERG1.2 belongs to a conserved gene family and is overexpressed and amplified in breast and ovarian cancer. Mol Carcinog 2003;38:188–200.
[55] Brunschwig EB, Wilson K, Mack D, et al. PMEPA1, a transforming growth factor-beta-induced marker of terminal colonocyte differentiation whose expression is maintained in primary and metastatic colon cancer. Cancer Res 2003;63:1568–1575.
[56] Jiménez-Segovia A, Mota A, Rojo-Sebastián A, et al. Prostaglandin F(2α)-induced Prostate Transmembrane Protein, Androgen Induced 1 mediates ovarian cancer progression increasing epithelial plasticity. Neoplasia 2019;21:1073–1084.
[57] Wang B, Zhong J-L, Li H-Z, et al. Diagnostic and therapeutic values of PMEPA1 and its correlation with tumor immunity in pan cancer. Life Sci 2021;277:119452.
[58] Abou-Elella A, Gramlich T, Fritsch C, Gansler T. c-myc amplification in hepatocellular carcinoma predicts unfavorable prognosis. Mod Pathol 1996;9:95–98.
[59] Singha PK, Pandeswara S, Venkatachalam MA, Saikumar P. Abstract 3024: targeting TMEPAI/PMEPA1 inhibits triple negative breast cancer cell growth and metastasis by enhancing growth suppressive TGF-β signaling. Cancer Res 2016;76:3024.
[60] Ma W-L, Lai H-C, Yeh S, et al. Androgen receptor roles in hepatocellular carcinoma, fatty liver, cirrhosis and hepatitis. Endocr Relat Cancer 2014;21:R165–R182.

Keywords: HCC; oncogene; TGF-β signalling; genetically engineered mouse model; GEMM; immune exhaustion; TMEPAI; STAG1.
Received 5 April 2024; received in revised form 16 August 2024; accepted 30 August 2024; Available online 7 September 2024